WILEY-VCH

FULL PAPER

Predicting stable molecular structures for $(RNC)_2Au^IX$ complexes

Hassan Rabaâ[a], Mohamed Chiheb[a], Alan L. Balch[b], and Dage Sundholm*[c]

Abstract: Calculations have been performed at the MP2 and DFT levels for investigating the reasons for the difficulties in synthesizing di(isocyanide)gold(I) halide complexes. Three-coordinated gold(I) complexes of the type $(R_3P)_2Au^IX$ **(1)** can be synthesized, whereas the analogous isocyanide complexes $(RNC)_2Au^IX$ **(2)** are not experimentally known. The molecular structures of $(R_3P)_2Au^IX$ (X= Cl, Br and I) and $(RNC)_2Au^IX$ with X = halide, cyanide, nitrite, methylthiolate, and thiocyanate are compared and structural differences are discussed. Calculations of molecular properties elucidate which factors determine the strength of the gold-ligand interactions in $(RNC)_2Au^IX$. The linear bonding mode of RNC favors a T-shaped geometry instead of the planar Y-shaped trigonal structure of $(R_3P)_2Au^IX$ complexes that have been synthesized. An increased polarity of the Au-X bond in (**2**) leads to destabilization of the Y-shaped structure. Chalcogen-containing ligands or cyanide appear to be good X-ligand candidates for synthesis of $(RNC)_2Au^IX$ complexes.

Introduction

Three-coordinated gold(I) complexes of the type $(R_3P)_2Au^IX$ (X = halide or pseudohalide) (**1**) are chemically stable compounds that display strong photo-luminescence upon UV irradiation, whereas the analogous complexes of the type $(RNC)_2Au^IX$ (**2**) have not been synthesized.[1-10] A few compounds related to (**2**) such as the two-coordinated $(RNC)Au^IX$ compounds have been prepared and structurally characterized.[11-21] Schmidbaur *et al.*[14-17] and Balch *et al.*[11,12,18,19] have reported synthesis of $(RNC)Au^IX$ complexes with R groups including methyl, phenyl, cyclohexyl, mesityl and with X = halide, triflate or tetrafluoroborate. In the solid state, the $(RNC)Au^IX$ complexes usually form extended linear chains, because the gold valence orbitals in these complexes are left open for aggregation through aurophilic bonding leading to the infinite molecular chain with $d\pi$-$p\pi$ hybridization.[11,12,22] In the dimers, the interaction with the anionic ligand has a large contribution from the closed-shell electrophilic gold(I) centers,[23-26] whose strength is enhanced by relativistic effects[27-29] as generally for gold(I) complexes.[30-32] Numerous two- and three-coordinate gold(I) complexes are suitable for sensor applications since their absorption and emission spectra are sensitive to a range of environmental factors.[33-35,39] For example, some gold complexes of the types considered here have been shown to be sensitive to mechanical pressure and change their luminescence and structure upon grinding.[40,41] Other gold(I) complexes are sensitive to the presence of volatile organic vapors and undergo changes in their luminescence spectra when certain vapors are present.[9,10,42] Some gold(I) complexes can undergo temperature dependent reversible or irreversible changes in structure and luminescence.[40,43] The factors affecting the stability of two- and three-coordinate gold(I) complexes need to be understood at theoretical levels in order to assist in the development of new sensors of this type and to understand the balance of stability between two- and three-coordinate gold(I) compounds.

Here, we report computational studies at the second-order Møller-Plesset perturbation theory (MP2) and density functional theory (DFT) levels of theory on a series of neutral gold complexes such as $(R_3P)_2Au^IX$ (**1**), $(RNC)_2Au^IX$ (**2**), $(RNC)Au^IX$ (**3**), and $(R_3P)Au^IX$ (**4**) in order to elucidate the main electronic factors influencing the stability of compounds with three covalent bonds to gold. We have studied several $(RNC)_2Au^IX$ complexes with R = H or where R is an organic ligand such as methyl (Me), phenyl (Ph), triphenyl methyl (Ph_3C), or cyclohexyl (Cy). The anionic ligand (X) is generally a halogen, cyanide, or a nitrite group.

[a] Prof. H., Rabaâ
Department of Chemistry, ESCTM
University Ibn Tofail
P.O. Box 133, Kenitra 14000, Morocco
E-mail: hrabaa@yahoo.com
[b] Prof. A. L. Balch
Department of Chemistry
University of California Davis,
California 95616, USA
[c] Prof. D. Sundholm
Department of Chemistry
University of Helsinki
P.O. Box 55, FI-00014 Helsinki, Finland

Supporting information for this article is given via a link at the end of the document.

Complexes with anionic chalcogen moieties have also been investigated. Two-coordinate complexes, $[(RNC)_2Au^I]^+X^-$ complexes not been considered,[44] because of their ionic nature. The calculations provide geometrical and electronic structure information about the strength of the Au-Cl, Au-C and Au-P bonds and show how the gold-X interaction depends on the σ or π acceptor properties of the ligands. The spatial extents of the frontier orbitals of different molecular fragments were used for assessing the chemical stability of the complexes. Calculated atomic charges provide information about electrostatic interactions and charge transfer effects.

Results and Discussion

$(Ph_3P)_2Au^IX$ complexes: The MP2 optimized molecular structure of $(Ph_3P)_2Au^ICl$ is shown in Figure 1. The most relevant structural parameters of the $(Ph_3P)_2Au^IX$ complexes with X = Cl, Br, and I (**1a**), (**1b**) and (**1c**) are given in Table 1, where they are compared to available experimental data.[42] In the $(Ph_3P)_2Au^IX$ complexes with X = Cl, Br, and I, the Au-X distance increases from 2.39 Å to 2.66 Å reflecting the larger atomic radius of the heavier halogens, whereas the length of the Au-P bond of 2.26-2.28 Å and the P-Au-P angle of 120° are almost independent of the anion X. An almost trigonal coordination of the gold(I) center is obtained for the Y-shaped planar complexes. The calculated bond distances and bond angles agree with experimental data.[42]

The chemical bonding of (**1a**), (**1b**), and (**1c**) is most likely due to an polarization of the σ_{Ph3P} donor of the $(Ph_3P)_2Au^+$ moiety, which interacts with the anionic ligand X. The halogen charges are -0.73 to -0.79 *e* and the charge of the gold atom is 0.29-0.31 *e* for the three molecules. The P atoms are positively charged with atomic charges of 0.49-0.53 *e*. The strength of the $Au^{\delta+}$-$X^{\delta-}$ bond is governed by electrostatic attractions with the positive P and Au atoms via the $Au^IX \leftarrow\sigma_X$ donation and $Au^IX \rightarrow\pi_X$ back donation to the p orbitals of X. While gold(I) is frequently considered as a poor π-back-bonding metal, recent computational studies have shown that a significant degree of back-donation from gold(I) can occur, particularly in three-coordinate systems with two phosphine ligands that are significantly bent.[45]

The effects of the size of the phosphine ligand (L) in the $(R_3P)_2Au^IX$ complexes were examined by comparing molecular properties of the $(Ph_3P)_2Au^IX$ and $(H_3P)_2Au^IX$ complexes with X = Cl, Br, and I (**1d**), (**1e**), and (**1f**) calculated at the MP2 level of theory. The most relevant bond lengths and bond angles of the $(H_3P)_2Au^IX$ complexes are given in Table 2. Comparison of the optimized structures for L = H_3P and L = Ph_3P shows that the bond lengths, bond angles, and the atomic charges of P are slightly affected by the size of the phosphine ligand and the poor σ donor character of H.

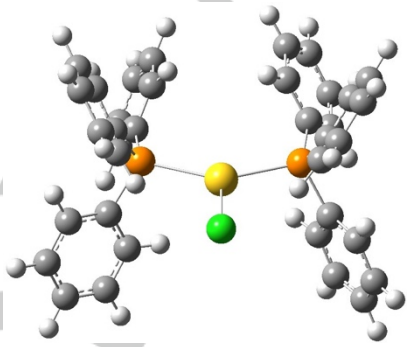

Figure 1. The molecular structure of $(Ph_3P)_2Au^ICl$ (**1a**) optimized at the MP2 level. The Cl atom is shown in green, Au in yellow, and the P atoms in orange. The C atoms of the phenyl groups are depicted in grey and the H atoms are light grey.

Table 1: Selected structural parameters for $(Ph_3P)_2Au^IX$ with X = Cl, Br, and I obtained by the molecular structure optimizations at the MP2 level of theory are compared to available experimental data**.** Distances are given in angstrom (Å) and angles in degree (°). Atomic charges (q in *e*) are also reported.

	$(Ph_3P)_2Au^ICl$ (**1a**)	$(Ph_3P)_2Au^IBr$ (**1b**)	$(Ph_3P)_2Au^II$ (**1c**)	$(Ph_3P)_2Au^ICl$ Exp.[42]
Au-X	2.394	2.519	2.660	2.522
Au-P	2.263; 2.267	2.271; 2.267	2.272; 2.275	2.322
P-Au-P	120	120	120	114
P-Au-X	121; 120	121; 119	120; 119	123
q_{Au}	0.31	0.30	0.29	
q_X	-0.79	-0.77	-0.73	
q_P	0.53	0.51	0.49; 0.50	

Table 2: Selected molecular structural parameters for $(H_3P)_2Au^IX$ with X=Cl, Br, and I optimized at the MP2 level of theory**.** Distances are given in Å and angles in degree (°). Atomic charges (q in *e*) are also reported.

	$(H_3P)_2Au^ICl$ (**1d**)	$(H_3P)_2Au^IBr$ (**1e**)	$(H_3P)_2Au^II$ (**1f**)
Au-X	2.398	2.526	2.665
Au-P	2.398; 2.359	2.238; 2.316	2.278; 2.278
P-Au-X	130; 88	120; 96	108;108
P-Au-P	142	144	143
q_{Au}	0.29	0.28	0.27
q_X	-0.79	-0.79	-0.76
q_P	0.30; 0.15	0.27; 0.19	0.22

The length of the Au-X bonds is almost the same for L_2Au^IX when L = H_3P as for the complex with L = Ph_3P, whereas the P-Au-P angle in $(H_3P)_2Au^ICl$ of 142° is significantly larger than the angle of 120° for $(Ph_3P)_2Au^ICl$. The van der Waals interactions between the phenyl groups reduce the P-Au-P angle, which might strengthen the Au-X bond as discussed below. Charge analysis shows that the phosphorus atoms are less positive for the complexes with L = H_3P than for L = Ph_3P. The covalent character of the Au-X bond is balanced by the electrostatic bonding of the negatively charged X and the positive L_2Au^I moiety.

$(RNC)_2Au^IX$ complexes: Synthesis of three-coordinated complexes of the type $(RNC)_2Au^IX$ (**2**) has not been reported in the literature, whereas molecules with cyclohexyl-isocyanide moieties coordinated to gold(I) as in $(CyNC)Au^IX$ have been synthesized and structurally characterized by X-ray diffraction.[11,12,14-17,18,19] The X-ray diffraction measurements for $(CyNC)Au^ICl$ show that in the solid state, the individual molecules form infinite chains with alternating aurophilic Au-Au bonding distances of 3.39 Å and 3.58 Å.[12] The $(CyNC)Au^IX$ complexes with X = Br and X = I crystallize in infinite chains with slightly longer Au-Au distances of 3.49-3.70 Å. The $(CyNC)Au^ICl$ (**3a)** complex shown in Figure 2 is used as reference structure for the hypothetical $(RNC)_2Au^IX$ (**2**) complexes with X = Cl, Br, and I. The experimental Au-C and Au-Cl distances in $(CyNC)Au^ICl$ are 1.96 Å and 2.26 Å, respectively,[12] which agree well with the values of 1.87 Å and 2.23 Å calculated at the MP2 level. Similar bond distances and bond angles were obtained at the MP2 level for $(RNC)Au^ICl$ with R = methyl (Me) (**3b**) and phenyl (Ph) (**3c**). Population analysis shows that the Cl atom in (**3a**)-(**3c**) is less negative than in (**1a**). The most relevant structural parameters of (**3b**)-(**3c**) listed in Table 3 agree well with the experimental data.

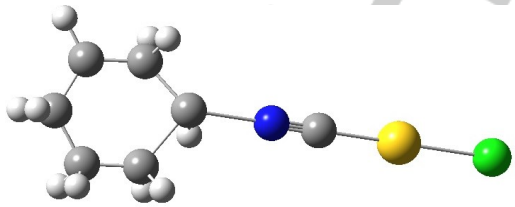

Figure 2: The molecular structure of the $(CyNC)Au^ICl$ (**3a**) optimized at the MP2 level of theory. The Cl atom is shown in green, Au in yellow, and the N atom in blue. Carbons and hydrogens are depicted in grey and light grey, respectively.

$(HNC)_2Au^IX$ complexes: The MP2 optimized molecular structure of the hypothetical $(HNC)_2Au^IX$ complexes with X = Cl (**2a**), Br, (**2b**) and I (**2c**) are shown in Figure 3. Relevant structural parameters are given in Table 4.

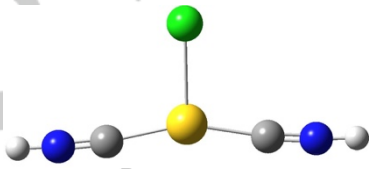

Figure 3: The molecular structure of the $(HNC)_2Au^ICl$ complex (**2a**) optimized at the MP2 level of theory. The Cl atom is shown in green, Au in yellow, N in blue, C in grey, and H in light grey.

Table 3: Selected molecular structural parameters for $(RNC)Au^ICl$ with R = cyclohexyl (Cy) (**3a**), methyl (Me) (**3b**) and phenyl (Ph) (**3c**) optimized at the MP2 level of theory compared with experimental data for $(CyNC)Au^ICl$. Distances are given in Å and angles in degree (°). Atomic charges (q in *e*) are reported.

	$(CyNC)Au^ICl$ (**3a**)	$(MeNC)Au^ICl$ (**3b**)	$(PhNC)Au^ICl$ (**3c**)	$(CyNC)Au^ICl$ Exp.[12]
Au-Cl	2.227	2.225	2.224	2.258
Au-C	1.870	1.869	1.863	1.961
q_{Au}	0.37	0.38	0.39	
q_{Cl}	-0.62	-0.61	-0.61	
q_C	-0.04	-0.02	-0.02	
q_N	0.16	0.00	0.05	

The calculations show that the Au-X distance in the bis-(alkylisocyanide)AuX complexes (**2a**), (**2b**) and (**2c**) increases from 2.42 Å in (**2a**) to 2.70 Å (**2c**). Thus, the Au-X distances are much longer in the three-coordinated complexes than the Au-Cl

distances of 2.22-2.23 Å for the two-coordinated complexes (**3a**), (**3b**) and (**3c**) given in Table 3.

The C-Au-C angle is 149-153° leading to a more open structure with a weaker Au-X bond than for the Y-shaped complex. The RNC ligand is a good σ donor and a weak π acceptor, whereas Cl is a π donor leading to a binding competition between the [HNC] and Cl^- ligands. The two [HNC] ligands make the Au-Cl bond more polar and weaker. The electrostatic repulsion is stronger because of the small electron back donation from gold(I) to [HNC]. The changes in the Au-X interaction can be traced back to the π bonding character of the first [HNC] ligand with gold(I) that lifts the energy levels of the 6s and 6p orbitals of Au, which leads to a weaker Au-Cl bond and favors the formation of an ionic $[(HNC)_2Au^I]^+X^-$ complex instead of stabilizing the three covalent gold-ligand bonds of the $(HNC)_2Au^IX$ complex.

Table 4: Selected molecular structural parameters for $(HNC)_2Au^ICl$ (**2a**), (**2b**), and (**2c**) with X=Cl, Br and I optimized at the MP2 level are given. Distances are given in Å and angles in degree (°). Atomic charges (q in *e*) are also reported.

	$(HNC)_2Au^ICl$ (**2a**)	$(HNC)_2Au^IBr$ (**2b**)	$(HNC)_2Au^II$ (**2c**)
Au-X	2.421	2.556	2.702
Au-C	1.926	1.937	1.938
C_1-Au-X	105	104	104
C_1-Au-C_2	149	152	153
q_{Au}	0.51	0.48	0.45
q_X	-0.80	-0.79	-0.76
q_C	0.01	0.01	0.01
q_N	-0.05	-0.04	-0.04

The stability of (**1**) and (**2**) can be also understood from the MO diagrams and the pictures of the frontier orbitals shown for the LAu^IX complexes in Figure 4. The HOMO of $(H_3P)Au^ICl$ is mainly localized to the Au-Cl bond, which is not unexpected since the Cl^- anion is a typical π donor. Addition of a second H_3P ligand to (**4a**) leads to a stable $(H_3P)_2Au^ICl$ complex, because the lowest unoccupied orbital (LUMO) of $(H_3P)Au^ICl$ interacts with the energetically nearly degenerate HOMO of the incoming H_3P moiety. The LUMO of (**3d**) has antibonding Au-Cl character. It is also much higher in energy than the HOMO of the incoming HNC moiety leading to an unstable $(HNC)_2Au^ICl$ (**2a**) complex.

Table 5: Selected molecular structural parameters for $(MeNC)_2Au^IX$ with X = CN^-, NO_2^-, F^-, Cl^- optimized at the MP2 level. Distances are given in Å and angles in degree (°). Atomic charges (q in *e*) are also reported.

	$(MeNC)_2Au^ICN$ (**2d**)	$(MeNC)_2Au^INO_2$ (**2e**)	$(MeNC)_2Au^IF$ (**2f**)	$(MeNC)_2Au^ICl$ (**2g**)	$(PhNC)_2Au^ICl$ (**2h**)
Au-X	2.041	2.280	2.119	2.462	2.491
Au-C	1.962; 1.988	1.903; 1.992	1.860; 2.066	1.935; 1.941	1.898; 1.972
C_1-Au-X	110	118	136	103	84
C_1-Au-C_2	132	161	151	156	160
C_2-Au-X	117	81	73	101	117
q_{Au}	0.50	0.46	0.52	0.48	0.49
q_X [a]	-0.72	-0.85	-0.87	-0.83	-0.82
q_C	-0.13; -0.11	-0.11; -0.05	0.04; -0.16	-0.07; -0.07	-0.13; -0.04
q_N	0.01; 0.00	0.09; 0.02	-0.04; 0.06	0.01; 0.02	-0.07; -0.06

[a] $q_C + q_N$ or $q_N + q_O + q_{O'}$ or q_F or q_{Cl}.

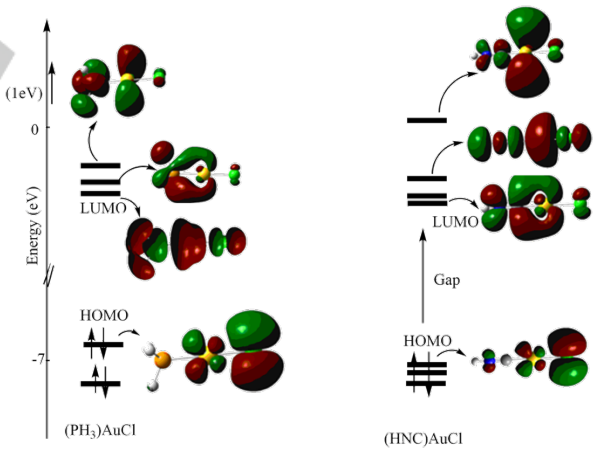

Figure 4: The frontier orbitals of the $(H_3P)Au^ICl$ (left) and $(HNC)Au^ICl$ (right) complexes calculated at the B3LYP level.

$(MeNC)_2Au^IX$ with X = CN^- NO_2^-, F^- and Cl^-: The stability of (**2**) with strong electron-donor and π acceptor ligands (X) and R = Me was assessed by investigating four $(MeNC)_2Au^IX$ complexes with

X = CN^- (**2d**), NO_2^- (**2e**), F^- (**2f**) and Cl^- (**2g**), where NO_2^- in (**2e**) is nitrogen bonded to Au. The molecular structure of $(MeNC)_2Au^INO_2$ is shown in Figure 5. The NO_2^- ligand stabilizes the 5d orbitals of gold(I) leading to a short Au-N bond distance of 2.280 Å.

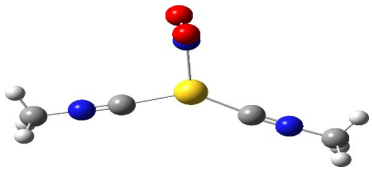

Figure 5: The molecular structure of $(MeNC)_2Au^INO_2$ **(2e)** optimized at the MP2 level of theory. The Au atom is shown in yellow, N in blue, C in grey, and H in light grey.

Selected bond lengths and bond angles of the optimized structures are given in Table 5. For (**2d**)-(**2f**), the calculations yield much shorter Au-X bond lengths of 2.04-2.28 Å than for (**2g**)-(**2h**) and (**2a**)-(**2c**) with X = Cl^-, Br^- and I^-. The Au-NO_2 distance in (**2e**) is about 0.2 Å shorter than the Au-Cl distance in (**2g**) of 2.46 Å. In (**2d**), the C-Au-C angle is 132° and the Au-X distance is also much shorter than for (**2g**) with X = Cl^-, which has a C-Au-C angle of 156° leading to an almost T-shaped structure. $(MeNC)_2Au^ICN$ (**2d**) has an almost perfect Y-shaped planar structure with three nearly identical Au-C distances, suggesting that it might be possible to synthesize the cyanide complex. Calculations on (**2d**) using the larger def2-TZVPP basis sets shows that almost the same bond distances and bond lengths are obtained with the two basis sets. The Au-C distances are 0.2-0.3 pm longer and the Au-Cl distance is 0.2 pm shorter when using the larger def2-TZVPP basis set. The C-Au-C angle is about one degree wider with the def2-TZVPP basis set. Calculations at the SCS-MP2/def2-TZVP level yielded 2.5 pm longer Au-C distances and 5 pm longer Au-Cl distance as obtained at the MP2/def2-TZVP level. The C-Au-C angle is about 3 degree wider at the SCS-MP2 level. These molecular structures agree well with the ones obtained at the default MP2/def2-TZVP level. The Au-X bonds are most likely shorter because CN^- and NO_2^- are better σ and π donors than Cl^-. The R and X ligands have to some extent a cooperative influence on the molecular structure. The differences in the stability originate mainly from the σ- and π-donor character of X to Au. The gold atom is more positively charged in the $(RNC)_2Au^IR'$ complexes than in $(R_3P)_2Au^IX$. The long Au-X distance shows that the Cl^- ligand is not a good donor, whereas with CN^- and NO_2^- the Au-X distance is much shorter indicating that X forms a stronger bond.

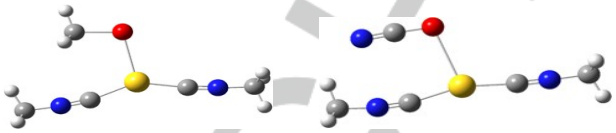

Figure 6: The molecular structure of (**2i**, left) and (**2j**) optimized at the MP2 level. The Au atom is shown in yellow, S in red, N in blue, C in grey, and H in light grey.

$(RNC)_2Au^ISMe$ and $(RNC)_2Au^ISCN$: Since thiolate ligands might stabilize three-coordinated gold compounds, we studied hypothetical sulfur-containing complexes like $(RNC)_2Au^ISR'$ with R' = Me or CN. Calculations on the $(MeNC)_2Au^ISMe$ (**2i**) complex show that the C-Au-C angle in (**2i**) of 142° is smaller than for (**2a**)-(**2c**) and (**2e**)-(**2h**), which suggests that it might be possible to synthesize thiolate complexes. Comparison of the molecular structures optimized at the MP2 and DFT levels show that dispersion effects slightly stabilize the sulfur-containing complexes, because the C-Au-C angle is smaller at the MP2 level than obtained at the B3LYP level. A σ_{Au-S} bond is formed in (**2i**). For $(MeNC)_2Au^ISCN$ (**2j**), the Au-S distance is much longer indicating that thiocyanate forms a weak Au-S bond. The molecular structures of (**2i**) and (**2j**) are shown in Figure 6 and the most important structural parameters are listed in Table 6.

Table 6: Selected molecular structural parameters for $(MeNC)_2Au^ISMe$ (**2i**) optimized at the MP2 and B3LYP levels of theory. Structural parameters for (**2j**) optimized at the MP2 level are also given. Distances are given in Å and angles in degree (°). Atomic charges (q in *e*) obtained at the B3LYP and Hartree-Fock levels are also reported.

	$(MeNC)_2Au^ISMe$ (**2i**) B3LYP	$(MeNC)_2Au^ISMe$ (**2i**) MP2	$(MeNC)_2Au^ISCN$ (**2j**) MP2
Au-S	2.439	2.365	2.498
$Au-C_1$ $Au-C_2$	2.083 1.993	1.970 1.930	1.970 1.923
C_1-Au-S C_2-Au-S	96 124	101 116	95 111
C_1-Au-C_2	140	142	155
q_{Au}	0.47	0.48	0.45
q_S	-0.54	-0.58	-0.50
q_C	-0.27; -0.19	-0.12; -0.11	-0.07; -0.14

In (**2i**), there is a strong interaction between the $[L_2Au^I]^+$ moiety and the methylthiolate ligand, which is also expected for sulfur-containing ligands. Thiolate complexes are more stable than the halogen complexes, because the energies of the p levels of sulfur are very close to the energies of the valence orbitals of gold, which leads to a stronger Au-ligand bond.

L_2Au^IX with bulky organic ligands: The influence of ligand-ligand interactions was studied by comparing the molecular structure of complexes with large organic ligands. The molecular structures of $(Ph_3CNC)_2Au^ICl$ (**2k**) is shown in Figure 7. Structural parameters obtained at the MP2 level for the gold-containing moiety of $(Ph)_3PAu^ICl$ (**4b**), $(PhNC)Au^ISMe$ (**3e**), $(PhNC)Au^ICl$ (**3c**), $(Ph_3P)_2Au^ICl]$ (**1a**), $(Ph_3CNC)_2Au^ICl$ (**2k**), and $(PhNC)_2Au^ISMe$ (**2l**) are compared in Table 7. Solvent effects corresponding to chloroform were modeled using the CPCM model.

The Au-X distances for (**4b**), (**3e**), and (**3c**) with one bulky organic ligand are in the range of 2.22-2.25 Å, which is much shorter than the Au-Cl distances for (**2k**) that have two RNC groups with bulky organic ligands. The Au-Cl distance of the (**1a**) complex is 2.39 Å. The C-Au-C angle of 166° is much wider for (**2k**) than the corresponding angle of 120° for (**1a**). The Au-Cl distance is further elongated by solvent effects that increase the ionic character of the $Au^{+\delta}$-$Cl^{-\delta}$ bond leading to a weakening of the bonding in (**2k**). Replacing Cl with SMe leads to a smaller C-Au-C angle of 145° and an Au-S distance of 2.36 Å, which indicates a higher stability for the sulfur-containing complex.

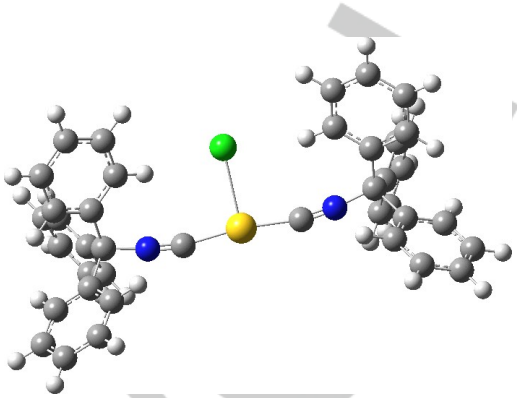

Figure 7: The molecular structure of $(Ph_3CNC)_2Au^ICl$ (**2k**) optimized at the MP2 level of theory. The Au atom is shown in yellow, P in orange, N in blue, Cl in green, C in grey, and H in light grey.

Table 7: The molecular structures of (**4b**), (**3e**), (**3c**), (**1a**), (**2k**), and (**2l**) calculated at the MP2 level. The bond lengths are given in Å and angles in degree (°).

	$(Ph_3P)Au^IXCl$ (**4b**)	$(PhNC)Au^ISMe$ (**3e**)	$(PhNC)Au^ICl$ (**3c**)	$(Ph_3CNC)_2Au^ICl$ (**2k**)	$(PhNC)_2Au^ISMe$ (**2l**)
Au-X	2.25	2.24	2.22	2.54	2.36
Au-P	2.18				
Au-C		1.89	1.86	1.93	1.92; 1.96
C-Au-C				166	145

Comparing orbitals of $(HNC)_2Au^ICl$ and $(H_3P)_2Au^ICl$: $(H_3P)_2Au^ICl$ (**1d**) and $(HNC)_2Au^ICl$ (**2a**) represent three-coordinated (140°) and the T-shaped (180°) complexes, respectively. For (**2d**), the highest occupied molecular orbitals (HOMOs) correspond to the five occupied d orbitals of gold(I). The HOMO of (**1d**) has a d_{z^2} character mixed with contributions from ligand orbitals. The HOMO energy of (**1d**) does not change when bending the molecule. The same holds for the lowest unoccupied molecular orbital (LUMO) which has significant Au_{6p} character, whereas the orbital with gold-ligand character is stabilized and becomes the LUMO of the bent (**1d**). The new LUMO is responsible for the binding of the second ligand of L_2Au^IX by providing a possibility for the second σ_{Au-L} bond. The HOMO of (**2a**) has d_{z^2} character and is destabilized when bending the molecule. The Au_{6p} orbital comes down in energy upon bending and it becomes the LUMO of the bent structure with a large energy gap to the d_{z^2} HOMO orbital. The different relative energies of the MOs

for the complexes with phosphine and isocyanide results in a linear structure for di(isocyanide)gold complexes (**2**), whereas the di(phosphine) complexes (**1**) are bent.

T-shaped and Y-shaped planar structures: Comparing the MO levels of the Y-shaped and T-shaped structures of L_2Au^IX shows that the P-Au-P or the C-Au-C angle plays an important role for gold-ligand interactions.[41] The planar trigonal Y-shaped and T-shaped structures of (**1**) and (**2**) belong locally approximately to the D_{3h} and C_{2v} point groups, respectively. The energy levels of the frontier orbitals of T-shaped and Y-shaped $[L\text{-}M\text{-}L]^+$ in Figure 8 show that the HOMO of $[(HCN)_2\ Au^I]^+$ is destabilized when bending the molecule, whereas for $[(H_3P)_2Au^I]^+$ the HOMO energy is almost independent of the L-Au-L angle. The HOMO of Y-shaped $[(H_3P)_2Au^I]^+$ has dominating contributions from the $5d_{xy}$, $5d_{x2-y2}$ orbitals on gold(I) leading to a bonding Au-L interaction, whereas the LUMO has a dominating $6p_z$ character that can form an Au-X bond. Molecular structure optimizations of the $(RNC)_2Au^IX$ (**2**) complexes lead to a T-shaped structure with a long Au-X distance, because the back donation from the $\pi/\pi*$ orbitals of the rigid RNC moiety to the 6p orbitals on gold(I) stabilizes the HOMO of the linear $[(RNC)_2Au^IX]^+$ structure leading to a weak Au-X bond.

Conclusions

Three-coordinated gold(I) complexes of the type $(RNC)_2Au^IX$ **(2)** have been studied computationally at the MP2 and DFT levels of theory. A series of models were constructed by varying the ligand R and the anion X in the $(RNC)_2Au^IX$ complexes in order to elucidate how electronic effects influence their stability. MO analyses show that the electrophilic closed-shell gold(I) centers interact strongly with phosphine and chlorine in the $(R_3P)_2Au^IX$ complexes but weakly with chlorine and RNC ligands in $(RNC)_2Au^ICl$. The reason for the stability of the $(R_3P)_2Au^IX$ complexes is the $Au^IX \leftarrow\sigma_X$ donation and the $Au^IX \rightarrow\pi_X$ back donation to the p orbitals of the halogen. The difference in the bonding between the $(RNC)_2Au^IX$ and $(Ph3P)_2Au^IX$ originates from the back donation from degenerate d orbitals to the $\pi/\pi*$ orbitals of RNC, which leads to a linear geometry for the $[(RNC)_2Au]^+$moiety and a weakly bond or unbound T-shaped $(RNC)_2Au^IX$ complex.

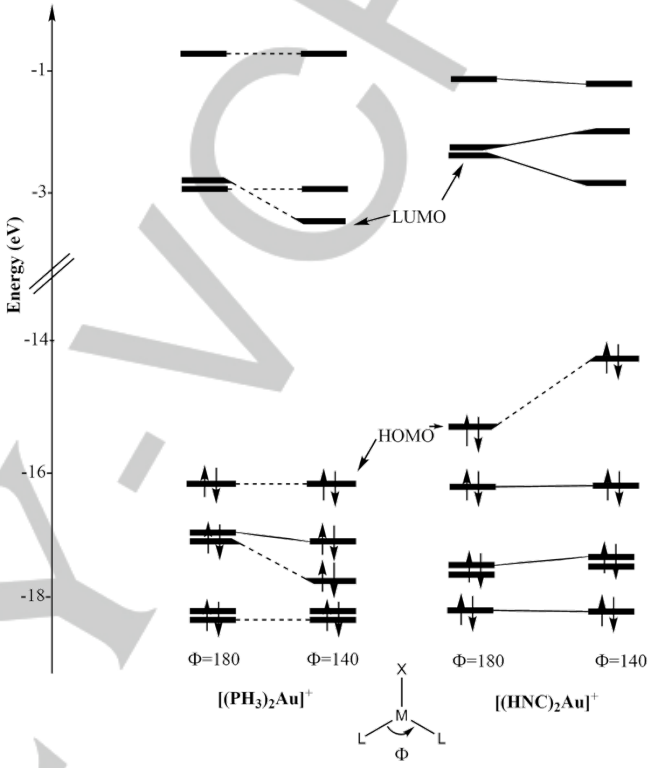

Figure 8: The energy levels of the frontier orbitals of the Y-shaped trigonal (Φ=140) and T-shaped (Φ=180) structures of the L_2Au^IX complexes.

Interactions of the gold(I) 6p orbital with the σ orbital of the second RNC moiety are thus needed for formation of $(RNC)_2Au^IX$ complexes. When the ionic character of the Au-X bond increases, the L-Au-L angle of the $(RNC)_2Au^IX$ complexes becomes wider leading to a destabilization and ultimately dissociation into its ionic parts. $(MeNC)_2Au^ICN$ might be synthesizable, since it has an almost perfect planar Y-shaped trigonal structure with three nearly identical Au-C distances. Chalcogen-containing X ligands also appear to be good candidates for obtaining stable $(RNC)_2Au^IX$ complexes. The Au-S bond in $(MeNC)_2Au^ISMe$ is found to be short thanks to the strong interaction between gold(I) and the sulfur-containing ligand. The main conclusions are based on the obtained molecular structures, whereas reaction pathways and energetics have not been accounted for in this work. The obtained

results might inspire experimentalists to try synthesizing the proposed $(RNC)_2Au^IX$complexes.

Experimental Section

The molecular structures were optimized at the second-order Møller-Plesset perturbation theory (MP2) level using the resolution of the identity approximation (RI-MP2)[46-48] as implemented in the Turbomole program package.[49] The Karlsruhe triple-ζ basis sets augmented with polarization functions (def2-TZVP) were used.[50] The basis-set convergence was assessed by performing MP2 calculations on $(MeNC)_2Au^ICl$ using the def2-TZVPP basis set with two *f* functions and one *g* function on Au.[42] Spin-component-scaled MP2 (SCS-MP2) was employed on $(MeNC)_2Au^ICl$, because MP2 tends to slightly overestimate interactions with Au.[43,51] Relativistic effects were accounted for by using the Stuttgart effective core potential (ECP) for gold and iodine.[52] The Cartesian coordinates of the molecular structures optimized at the MP2/def2-TZVP level are given as Supporting Information. The molecular structures were also optimized at the density functional theory level using the B3LYP functional[53,54] and the def2-TZVP basis sets. Harmonic frequencies were calculated in order to verify that the obtained stationary points are minima on the potential energy surface. The molecular orbital diagrams were calculated with the Gaussian 09 program package[55] using the def2-TZVP basis sets for the light atoms and the LANL2DZ ECP[56] and the corresponding basis set for gold and iodine. Singlet spin states were assumed and no symmetry constraints were imposed. Atomic charges were calculated at the Hartree-Fock and B3LYP levels using the population analysis based on occupation numbers (PABOON) as implemented in Turbomole.

In order to estimate the stability of the computed complexes under experimental conditions, solvent effects corresponding to chloroform were modeled at the MP2 level by using the polarizable conductor calculation model (CPCM) as implemented in Gaussian 09.[57,58]

Acknowledgments

H.R. acknowledges support from the University of Helsinki, University of California, Davis, and the European Commission through H2020 project (MSCA-RISE-2016- 734759-VAHVISTUS. We thank Prof. R. Hoffmann (Cornell University), Prof. M.A. Omary, (University of North Texas) and Prof. P. Pyykkö (University of Helsinki) for discussion. This work was supported by The Academy of Finland (project 275845) and Magnus Ehrnrooth Foundation. The Finnish IT Center for Science (CSC) is acknowledged for computational resources.

Keywords: ab initio calculations, density functional calculations, gold, molecular modeling, structure elucidation

[1] L. Malatesta, L. Naldini, G. Simonetta, F. Cariati, *Coord. Chem. Rev*., **1966,** *1*, 255-289.

[2] R. Ziolo, S. Lipton, Z. Dori, *Chem. Comm*., **1970**, 1124-1125.

[3] T. M. McCleskey, H. B. Gray, *Inorg. Chem.,* **1992**, *31*, 1733-1734.

[4] C. King, M. N. I. Khan, R. J. Staples, J. P. Fackler, Jr., *Inorg. Chem.,* **1992**, *31,* 3236-3238.

[5] M. Hoshino, H. Uekusa, Y. Ohashi, *Bull. Chem. Soc. Jpn.,* **2006**, *79*, 1362-1366.

[6] M. Hoshino, H. Uekusa, S. Sonoda, T. Takuhiro Otsuka, Y. Kaizu, *Dalton Trans.*, **2009**, 3085–3091.

[7] M. Hoshino, H. Uekusa, S. Ishii, T. Otsuka, Y. Kaizu, Y. Ozawa, K. Toriumi, *Inorg. Chem.* **2010***, 49*, 7257–7265.

[8] P. Sinha, A. K. Wilson, M. A. Omary, *J. Am. Chem. Soc*., **2005**, *127*, 12488-12489.

[9] S. H. Lim, M. M. Olmstead, A. L. Balch, *J. Am. Chem. Soc*., **2011**, *133*, 10229-10238.

[10] S. H. Lim, M. M. Olmstead, A. L. Balch, *Chem. Sci.*, **2013**, *4*, 311-318.

[11] O. Elbjeirami; M. A. Omary, M. Stender, A. L. Balch, *Dalton Trans.,* **2004**, 3173-3175.

[12] R. L. White-Morris, M. M. Olmstead, A. L. Balch, O. Elbjeirami, M. A. Omary, *Inorg. Chem.,* **2003**, *42,* 6741-6748.

[13] R.-Y Liau; T. Mathieson; A. Schier; R. J. F. Berger; N. Runeberg; H. Schmidbaur, *Naturforsch.,* **2002**, *57b*, 881-889.

[14] H. Schmidbaur, *Nature*, **2001**, *413*, 31-32.

[15] W. Schneider, A. Sladek, A. Bauer, K. Angermaier and H. Schmidbaur, *Z. Naturforsch.,* **1997**, *52b*, 53-56.

[16] J. E. D. T. Wilton-Ely, A. Schier, H. Schmidbaur. *Organometallics,* **2001**, *20,* 1895-1897.

[17] A. Grohmann, H. Schmidbaur, in *Comprehensive Organometallic Chemistry II*, (Eds. E. W. Abel, F. Stone, G. Wilkinson), Elsevier, Oxford, **1995**, vol. *3*, p. 1.

[18] J. E. Parks, A. L. Balch, *J. Organomet. Chem.,* **1974**, *71,* 453-463.

[19] R. L. White-Morris, M. M. Olmstead, A. L. Balch, *J. Am. Chem. Soc.,* **2003**, *125*, 1033-1040.

[20] S. M. Humphrey, H.-G. Mack, C. Redshaw, M. R. J. Elsegood, K. J. H. Young, H. A. Mayer, W. C. Kaska, *Dalton Trans.,* **2005**, 439-446.

[21] U. Siemeling, D. Rother, C. Bruhn, H. Fink, T. Weidner, F. Traeger, A. Rothenberger, D. Fenske, A. Priebe, J. Maurer, R. Winter, *J. Am. Chem. Soc.,* **2005**, *127*, 1102-1103.

[22] T. J. Mathieson, A. G. Langdon, N. B. Milestone, B. K. Nicholson. *Dalton Trans.,* **1999**, 201-207.

[23] W. B. Jones, J. Yuan, R. Narayanaswany, M. A.Young, R. C. Elder, A. E. Bruce, M. R. M. Bruce, *Inorg. Chem*., **1995**, *34*, 1996-2001.

[24] a) J. C. Vickery, M. M. Olmstead, E. Y. Fung, A. L. Balch, *Angew. Chem. Int. Ed.*, **1997**, *36*, 1179-1181. b) A. Marchenko, G. Koidan, A. Hurieva, Y. Vlasenko, A. Kostyuk, A. Lenarda, A. Biffis, C. Tubaro, M. Baron, C. Graiff, F. Nestola, *J. Orgometal. Chem*., **2017**, *829*, 71-78.

[25] S. S. Pathaneni, G. R. Desiraju, *J. Chem. Soc. Dalton Trans.,* **1993**, 319-323.

[26] H. Schmidbaur, W. Graf, G. Müller, *Angew. Chem. Int. Ed. Engl.,* **1988**, *27*, 417-419.

[27] P. Pyykkö, N. Runeberg, F. Mendizabal, *Chem. Eur. J.,* **1997***, 3*, 1451-1453.

[28] P. Pyykkö*, Chem. Soc. Rev*., **2008**, *37*, 1967-1997.

[29] K. M. Merz, Jr., R. Hoffmann, *Inorg. Chem*., **1988**, *27*, 2120-2127.

[30] R. Hoffmann, *Angew. Chem. Internat. Ed*., **1982**, *21*, 711–724.

[31] H. Rabaâ, A. S. K. Hashmi, B. Engels, T. Hupp, *Int. J. Quant. Chem.,* **2007**, *107*, 359-365.

[32] H. Rabaâ, K. Barakat, M. A. Omary, T. R. Cundari, *J. Phys. Chem***.** B**, 2006**, *110*, 14645-14651 and references therein**.**

[33] V. W.-W Yam, V. K-M. Au, S.Y.-L Leung. *Chem. Rev*., **2015**, *115*, 7589-7728.

[34] O. S. Wenger, *Chem. Rev*., **2013**, *113,* 3686-3733.

[35] M. A. Mansour, W. B. Connick, R. J. Lachicotte, H.J. Gysling, R. Eisenberg, *J. Am. Chem. Soc.,* **1998***, 120*, 1329-1330.

[36] A. Burini, J. P. Fackler, Jr., R. Galassi, T.A. Grant, M. A. Omary, A. Rawashdeh-Omary, B. R. Pietroni, R. J. Staples, *J. Am. Chem. Soc.,* **2000**, *122*, 11264-11264.

[37] D. Schneider, O. Schuster, H. Schmidbaur, *J. Chem. Soc. Dalton Trans.,* **2005**, 1940-1947.

[38] D. Schneider, A. Schier, H. Schmidbaur, *J. Chem. Soc. Dalton Trans.,* **2004**, 1995-2005.

[39] D. E. Harwell, M. D. Mortimer, C. B. Knobler, F. A. L. Anet, M. F. Hawthorne, *J. Am. Chem. Soc.,* **1996**, *118*, 2679-2685.

[40] Y. A. Lee, R. Eisenberg, J. Am. Chem. Soc. **2003**, *125*, 7778-7779.

[41] D. T. Walters, R. B. Aghakanpour, X. B. Powers, K. B. Ghiassi, M. M. Olmstead, A. L. Balch, *J. Am. Chem. Soc*., **2018**, *140*, 7533-7542.

[42] M. A. Malwitz, S. H. Lim, R. L. White-Morris, D. L. Pham, M. M. Olmstead, A. L. Balch*, J. Am. Chem. Soc*., **2012,** *134*, 10838-10839.

[43] E. M. Gussenhoven, J. C. Fettinger, D. M. Pham, M. M. Malwitz, A. L. Balch*, J. Am. Chem. Soc*. **2005** *127*, 10838-10839

[44] J.Yau, D. M. P. Mingos, *J. Chem. Soc. Dalton Trans*. **1997**, 1103-1112; F. Bonati, G. Minghetti, Gazz. Chim. Ital. **1973**, *103*, 373-386; G. Minghetti, L. Baratto, F. Bonati, *J. Organometal. Chem*. **1975**, *102*, 397-406; J. A. McCleerty, M. M. M. da Mota, *J. Chem. Soc. Dalton Trans.* **1973**, 2571-2574.

[45] M. Joost, L. Estévez, S. Mallet-Ladeira, K. Miqueu, A. Amgoune, D. Bourissou, *Angew. Chem. Int. Ed*. **2014**, *53*, 14512 -14516; L. Nunes dos Santos Comprido, J. E. M. N. Klein, G. Knizia, J. Kïstner, A. S. K. Hashmi, *Chem. Eur. J*. **2016**, *22*, 2892-2895.

[46] D. Feller, E. D. Glendening, D. E. Woon, M. W. Feyereisen, *J. Chem. Phys.,* **1995**, *103,* 3526-3542.

[47] F. Weigend, M. Häser, *Theor. Chim. Acc.,* **1997**, *97*, 331-340.

[48] A. Schäfer, C. Huber, R. Ahlrichs, *J. Chem. Phys*., **1992,** *97*, 2571-2577.

[49] R. Ahlrichs, M. Bär, M. Häser, H. Horn, C. Kölmel, *Chem. Phys. Lett*., **1989**, *162*, 165-169.

[50] F. Weigend, *Phys. Chem. Chem. Phys*., **2006**, *8*, 1057-1065.

[51] M. Gerenkamp, S. Grimme, *Chem. Phys. Letters*, **2004**, *392*, 229-235.

[52] D. Figgen, K. A. Peterson, M. Dolg, H. Stoll, *J. Chem. Phys.,* **2009**, *130*, 164108.

[53] A. D. Becke, *Phys. Rev. A*, **1988**, *38*, 3098-3100.

[54] A. D. Becke, *J. Chem. Phys*., **1993**, *98*, 5648-5652.

[55] M. J. Frisch, *et al*., Gaussian 09, Revision, A. I. Gaussian, Inc., Wallingford CT. **2009**.

[56] P. J. Hay, W.R. Wadt, *J. Chem. Phys*., **1985**, *82*, 270-283.

[57] A. Klamt, G. Schurmann, *J. Chem. Soc., Perkin Trans. 2*, **1993**, 799-805.

[58] J. Andzelm, C. Kölmel, A. Klamt, *J. Chem. Phys*., **1995**, *103*, 9312-9320.

Entry for the Table of Contents

FULL PAPER

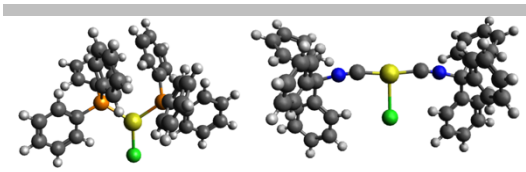

The underlying reasons for the difficulties to synthesize $(RNC)_2Au^IX$ complexes are computationally investigated. The optimized molecular structures of the $(RNC)_2Au^IX$ and $(R_3P)_2Au^IX$ complexes with X = halide, cyanide, nitrite, methylthiolate, and thiocyanate moieties are compared and the structural differences are discussed.

Key Topic Gold chemistry

Authors:

Hassan Rabaâ, Mohamed Chiheb, Alan L. Balch, and Dage Sundholm*

Page 1. – Page 9.

Title: Predicting stable molecular structures for $(RNC)_2Au^IX$ complexes

[a] Prof. H., Rabaâ
Department of Chemistry, ESCTM
University Ibn Tofail
P.O. Box 133, Kenitra 14000, Morocco